Zirconium Complexes of Fluorinated Aryl Diamides

Paul E. O'Connor, Darryl J. Morrison, Sheryl Steeves, Katherine Burrage, and David J. Berg*

Department of Chemistry, University of Victoria, P.O. Box 3065, Victoria, British Columbia, Canada V8W 3V6

Received July 31, 2000

The reaction of excess Ar^FNHLi with $(ICH_2CH_2OCH_2)_2$ affords the new diamines $(Ar^FNHCH_2CH_2OCH_2)_2$ (**1**, $Ar^F = C_6F_5$; **2**, $Ar^F = 3,5\text{-}C_6H_3(CF_3)_2$) in moderate yield. Direct protonolysis of $Zr(CH_2Ph)_nCl_{4-n}$ ($n = 2-4$) or $Zr[N(SiMe_3)_2]_nCl_{4-n}$ ($n = 2, 3$) with **1** or **2** (1 equiv) affords the zirconium complexes $Zr(Ar^FNCH_2CH_2OCH_2)_2(X)(Y)$ ($Ar^F = C_6F_5$: **3**, X = Y = Cl; **4**, X = $N(SiMe_3)_2$, Y = Cl; **5**, X = Cl, Y = CH_2Ph; **6**, X = Y = CH_2Ph. $Ar^F = 3,5\text{-}C_6H_3(CF_3)_2$: **7**, X = Y = Cl; **8**, X = Y = CH_2Ph). The structures of **1**, **4**, **5**, and **7** were established by X-ray crystallography with the zirconium complexes **4**, **5**, and **7** all adopting a monocapped trigonal bipyramidal geometry in the solid state. However, in solution, these complexes display higher symmetry due to rapid ligand rearrangement. The silylamido complex **4** shows restricted rotation of the C_6F_5 rings in solution ($\Delta G^{\ddagger} = 49 \pm 3$ kJ mol^{-1}). Abstraction of a benzyl group from **6** by $B(C_6F_5)_3$ affords $\{Zr[CH_2OCH_2CH_2N(C_6F_5)]_2(CH_2Ph)\}^+\{(PhCH_2)B(C_6F_5)_3\}^-$ (**9**). This complex shows evidence for η^2-benzyl coordination and does not polymerize ethylene at room temperature. Treatment of **3** with excess MAO (500 equiv) and ethylene (1 atm, 50 °C) affords polyethylene at a modest rate (3.2 kg mol^{-1} Zr h^{-1}).

Introduction

The past decade has witnessed rapid development in the use of non-cyclopentadienyl ligand systems for group 4 organometallic chemistry.[1−4] Much of this effort has been directed at the development of new olefin polymerization catalysts, and a number of nitrogen-based ligand systems have been successfully employed for this application.[2−4] Of particular note, zirconium alkyl cations supported by chelating diamido ligands have been found to function as high activity, living polymerization catalysts for ethylene and 1-hexene.[3,4]

In previous work, we reported the synthesis of a number of zirconium dialkyls *cis*- and *trans*-Zr(DAC)R_2, their corresponding alkyl cations $Zr(DAC)R^+$, and the isoelectronic yttrium alkyls Y(DAC)R, supported by the chelating diamido macrocycle, deprotonated 4,13-diaza-18-crown-6 (DAC^{2-}).[5,6] While these complexes displayed interesting chemistry with alkynes, they showed no tendency to insert alkenes into the metal−carbon bonds. This result was attributed to electronic factors since all of our earlier results suggested that the DAC ligand was the steric equivalent of two C_5Me_5 groups.[5,6] Therefore, to increase metal−carbon reactivity, we decided to decrease the number and strength of the donors present in the ligand framework. This has been accomplished by removing two of the four DAC ether donors and substituting the amido nitrogens with strongly electron-withdrawing fluorinated aryl groups in the new ligands $[Ar^FNCH_2CH_2OCH_2]_2^{2-}$ ($Ar^F = C_6F_5$, $3,5\text{-}C_6H_3(CF_3)_2$). In this contribution we report the

* To whom correspondence should be addressed.

(1) Leading references can be found in: (a) Vollmerhaus, R.; Rahim, M.; Tomaszewski, R.; Xin, S.; Taylor, N. J.; Collins, S. *Organometallics* **2000**, *19*, 2161. (b) Martin, A.; Uhrhammer, R.; Gardner, T. G.; Jordan, R. F.; Rogers, R. D. *Organometallics* **1998**, *17*, 382.

(2) (a) Horton, A. D.; de With, J. *Chem. Commun.* **1996**, 1375. (b) Cloke, F. G. N. Geldbach, T. J.; Hitchcock, P. B.; Love, J. B. *J. Organomet. Chem.* **1996**, *506*, 343. (c) Clark, H. C. S.; Cloke, F. G. N.; Hitchcock, P. B.; Love, J. B.; Wainright, A. P. *J. Organomet. Chem.* **1995**, *501*, 333. (d) Aoyagi, K.; Gantzel, P. K.; Kalai, K.; Tilley, T. D. *Organometallics* **1996**, *15*, 923. (e) Hermann, W. A.; Denk, M.; Albach, R. W.; Behm, J.; Herdtweck, E. *Chem. Ber.* **1991**, *124*, 683. (f) Gibson, V. C.; Kimberley, B. S.; White, A. J. P.; Williams, D. J.; Howard, P. *Chem. Commun.* **1998**, 313. (g) Male, N. A. H.; Thornton-Pett, M.; Bochmann, M. *J. Chem. Soc., Dalton, Trans.* **1997**, 2487. (h) Kempe, R.; Brenner, S.; Arndt, P. *Organometallics* **1996**, *15*, 1071. (i) Tsuie, B.; Swenson, D. C.; Jordan, R. F.; Petersen, J. L. *Organometallics* **1997**, *16*, 1392. (j) Tinkler, S.; Deeth, R. J.; Duncalf, D. J.; McCamley, A. *Chem. Commun.* **1996**, 2623.

(3) (a) Scollard, J. D.; McConville, D. H.; Vittal, J. J. *Organometallics* **1995**, *14*, 5478. (b) Scollard, J. D.; McConville, D. H.; Vittal, J. J. *Organometallics* **1997**, *16*, 4415. (c) Scollard, J. D.; McConville, D. H.; Vittal, J. J. *Macromolecules* **1996**, *29*, 5241. (d) Scollard, J. D.; McConville, D. H. *J. Am. Chem. Soc.* **1996**, *118*, 10008. (e) Guerin, F.; McConville, D. H.; Vittal, J. J. *Organometallics* **1996**, *15*, 5586.

(4) (a) Aizenberg, M.; Turculet, L.; Davis, W. M.; Schattenmann, F.; Schrock, R. R. *Organometallics* **1998**, *17*, 4795. (b) Schattenmann, F.; Schrock, R. R.; Davis, W. M. *Organometallics* **1998**, *17*, 989. (c) Schrock, R. R.; Seidel, S. W.; Schrodi, Y.; Davis, W. M. *Organometallics* **1999**, *18*, 428. (d) Graf, D. D.; Schrock, R. R.; Davis, W. M.; Stumpf, R. *Organometallics* **1999**, *18*, 843. (e) Flores, M. A.; Manzoni, M.; Baumann, R.; Davis, W. M.; Schrock, R. R. *Organometallics* **1999**, *18*, 3220. (f) Schrock, R. R.; Baumann, R.; Reid, S. M.; Goodman, L. T.; Stumpf, R.; Davis, W. M. *Organometallics* **1999**, *18*, 3649. (g) Liang, L.-C.; Schrock, R. R.; Davis, W. M. *Organometallics* **2000**, *19*, 2526. (h) Baumann, R.; Davis, W. M.; Schrock, R. R. *J. Am. Chem. Soc.* **1997**, *119*, 3830. (i) Baumann, R.; Stumpf, R.; Davis, W. M.; Liang, L.-C.; Schrock, R. R. *J. Am. Chem. Soc.* **1999**, *121*, 7822 (j) Schrock, R. R.; Schattenmann, F.; Aizenberg, M.; Davis, W. M. *Chem. Commun.* **1998**, 199. (k) Schrock, R. R.; Lee, J.; Liang, L.-C.; Davis, W. M. *Inorg. Chim. Acta* **1998**, *270*, 353. (l) Baumann, R.; Schrock, R. R. *J. Organomet. Chem.* **1998**, *557*, 69. (m) Schrock, R. R.; Liang, L.-C.; Baumann, R.; Davis, W. M. *J. Organomet. Chem.* **1999**, *591*, 163.

(5) Lee, L.; Berg, D. J.; Bushnell, G. W. *Organometallics* **1997**, *16*, 2556.

(6) (a) Lee, L.; Berg, D. J.; Einstein, F. W.; Batchelor, R. J. *Organometallics* **1997**, *16*, 1819. (b) Lee, L.; Berg, D. J.; Bushnell, G. W. *Organometallics* **1995**, *14*, 5021. (c) Lee, L.; Berg, D. J.; Bushnell, G. W. *Organometallics* **1995**, *14*, 8.

10.1021/om0006559 CCC: $20.00
Publication on Web 02/23/2001

synthesis and structural studies on several zirconium complexes containing these ligands. In addition, the formation of a cationic zirconium alkyl complex and the reactivity of these complexes as precatalysts for olefin polymerization are discussed.

It should be pointed out that Schrock's group has reported closely related group 4 complexes of NON and NSN ligand systems that possess a single ether[4a,e−i,l−m] or thioether[4a,d] donor in the backbone, but without the fluorinated aryl substituents on the amido nitrogen. Many of these complexes polymerize or oligomerize olefins and provide an interesting comparison to those reported here.

Experimental Section

General Procedures. All manipulations were carried out under an argon atmosphere, with the rigorous exclusion of oxygen and water, using standard glovebox (Braun MB150-GII) or Schlenk techniques. Tetrahydrofuran (THF), hexane, and toluene were dried by distillation from sodium benzophenone ketyl under argon immediately prior to use. Tetrabenzylzirconium,[7] $Zr[N(SiMe_3)_2]_3Cl$,[8] and $Zr[N(SiMe_3)_2]_2Cl_2$[8] were prepared according to literature procedures. Tribenzylzirconium chloride and dibenzylzirconium dichloride were prepared from zirconium tetrachloride and benzylmagnesium chloride by appropriate modification of the tetrabenzylzirconium synthesis.[7] $B(C_6F_5)_3$ was a generous gift from Boulder Scientific and was purified by stirring with Me_2SiCl_2 followed by vacuum sublimation. Pentafluoroaniline, 3,5-bis(trifluoromethyl)aniline, 1,2-bis(2-chloroethoxy)ethane, *n*-butyllithium, and MAO were obtained commercially (Aldrich) and were used as received. 1,2-Bis(2-iodoethoxy)ethane was prepared by refluxing 1,2-bis(2-chloroethoxy)ethane with NaI in acetone according to a literature procedure.[9]

^1H (360 MHz), ^{13}C (90.55 MHz), ^{19}F (338.86 MHz), ^{29}Si (71.54 MHz), ^{11}B (115.54 MHz), and all variable-temperature NMR spectra were recorded on a Bruker AMX-360 MHz spectrometer. All deuterated solvents were dried over activated 4 Å molecular sieves, and spectra were recorded using 5 mm tubes fitted with a Teflon valve (Brunfeldt) at room temperature unless otherwise specified. ^1H and ^{13}C NMR spectra were referenced to residual solvent resonances. ^{19}F NMR spectra were referenced to external CCl_3F, ^{29}Si NMR spectra were referenced to external TMS, and ^{11}B spectra were referenced to external $BF_3(OEt_2)$ (0.1 M in $CDCl_3$). For most compounds, proton and carbon NMR assignments were confirmed by $^1H-^1H$ or $^1H-^{13}C$ COSY experiments. Melting points were recorded using a Büchi melting point apparatus and are not corrected. Elemental analyses were performed by Canadian Microanalytical, Delta, B.C. Despite the use of cooxidants such as V_2O_5 and PbO_2, the analytical data for most complexes were consistently 1−3% low in carbon. This may be due to metal carbide formation. Mass spectra were recorded on a Kratos Concept H spectrometer using electron impact (70 eV) or FAB methods.

$[CH_2OCH_2CH_2NH(C_6F_5)]_2$ (1). Pentafluoroaniline (5.82 g, 31.8 mmol) was weighed into a large Schlenk flask and dissolved with stirring in 100 mL of dry THF under argon. The solution was cooled to −78 °C with an acetone−dry ice bath, and 20 mL of 1.6 M *n*-BuLi (32 mmol) was added via syringe. The dark red solution was stirred for 10 min, and bis(2-iodoethoxy)ethane (2.96 g, 8.00 mmol) was added by dropping funnel over a 30 min period. The solution was allowed to warm to room temperature over a 1 h period and was then refluxed overnight. The THF solvent was removed under reduced pressure, and the residue was redissolved in diethyl ether. Water was carefully added, and the dark red organic phase was separated and dried over anhydrous $MgSO_4$. After filtration, the ether solution was reduced in volume to ca. 2 mL and transferred to a short-path distillation apparatus. The remaining ether was removed, and the residue was heated at 120 °C (10^{-1} mmHg) to distill off all remaining pentafluoroaniline. The black tarry residue was extracted with diethyl ether and taken to dryness. Repeated recrystallization from hot hexane yielded very pale yellow crystals. Yield: 63%. Mp: 62−4 °C. NMR (d_6-benzene): ^1H δ 3.81 (br s, 2H, N*H*), 3.13 (m, 4H, CH_2O), 3.085 (m, 4H, CH_2N), 3.077 (m, 4H, CH_2O); $^{13}C\{^1H\}$ (d_6-benzene) δ 138.4 (d, *m*-aryl*C*, $^1J_{CF} = 249$ Hz), 133.7 (d, *p*-arylC, $^1J_{CF} = 244$ Hz), 127.3 (*quat*-aryl*C*), 125.8 (d, *o*-aryl*C*, $^1J_{CF} = 255$ Hz), 70.3 (NCH$_2$CH$_2$O), 69.7 (OCH$_2$CH$_2$O), 45.8 (NCH$_2$CH$_2$O); $^{19}F\{^1H\}$ (*d*-chloroform) δ −160.3 (dd, *o*-aryl*F*, $^3J_{FF} = 22.5$ Hz, $^4J_{FF} = 7.5$ Hz), −166.0 (br t, *m*-aryl*F*, $^3J_{FF} = 22.5$ Hz), −175.2 (tt, *p*-aryl*F*, $^3J_{FF} = 22.5$ Hz, $^4J_{FF} = 7.5$ Hz). High res. MS (EI) found (calcd): M^+ 480.0883 (480.0896).

$[CH_2OCH_2CH_2NH(3,5\text{-}C_6H_3(CF_3)_2)]_2$ (2). This compound was prepared by the procedure outlined for **1** above using bis(3,5-trifluoromethyl)aniline. Yield: 40%. Mp: 58−60 °C. NMR (*d*-chloroform): ^1H δ 7.15 (s, 2H, *p*-arylC*H*), 6.90 (s, 4H, *o*-arylC*H*), 4.58 (br s, 2H, N*H*), 3.77 (m, 4H, NCH$_2$CH_2O), 3.70 (s, 4H, OCH_2CH_2O), 3.35 (m, 4H, CH_2N); $^{13}C\{^1H\}$ δ 148.5 (*quat*-aryl*C*), 132.4 (q, *m*-aryl*C*, $^2J_{CF} = 37$ Hz), 123.5 (q, *C*F$_3$, $^1J_{CF} = 276$ Hz), 112.3 (*o*-aryl*C*), 110.6 (*p*-aryl*C*), 70.3 (NCH$_2$*C*H$_2$O), 69.2 (OCH_2*C*H$_2$O), 43.3 (NCH_2CH$_2$O); $^{19}F\{^1H\}$ δ −63.0 (C*F*$_3$). High res MS (FAB) found (calcd): $M^+ + 1$ 573.1419 (573.1412).

$Zr[CH_2OCH_2CH_2N(C_6F_5)]_2Cl_2$ (3). A solution of **1** (0.100 g, 0.208 mmol) in 4 mL of toluene was added to a suspension of $Zr[N(SiMe_3)_2]_2Cl_2$ (0.100 g, 0.208 mmol) in 16 mL of toluene, and the reaction mixture was heated at 110 °C for 2 days. Complex **3** precipitated directly from the reaction mixture on cooling and was obtained as an analytically pure powder after washing with hexane and drying under vacuum. Alternatively, **3** can be obtained in similar yield and purity by mixing equimolar quantities of **1** and $Zr(CH_2Ph)_2Cl_2$ at room temperature. Yield: 90%. Mp: 231−2 °C. NMR (d_5-bromobenzene): ^1H δ 4.04 (br s, 4H, NCH$_2$CH_2O), 3.84 (s, 4H, OCH_2CH_2O), 3.80 (br s, 4H, NCH_2CH$_2$O); $^{13}C\{^1H\}$ δ 71.5 (NCH$_2$*C*H$_2$O), 69.9 (OCH$_2$*C*H$_2$O), 53.2 (NCH$_2$CH$_2$O); $^{19}F\{^1H\}$ δ −148.4 (d, *o*-aryl*F*, $^3J_{FF} = 22.4$ Hz), −164.1 (t, *p*-aryl*F*, $^3J_{FF} = 22.4$ Hz), −170.2 (br s, *m*-aryl*F*). ^1H NMR (d_6-benzene): δ 3.58 (br s, 4H, NCH$_2$CH_2O), 3.48 (br s, 4H, NCH_2CH$_2$O), 3.07 (s, 4H, OCH_2CH_2O). Anal. Calcd for $C_{18}H_{12}N_2O_2F_{10}Cl_2Zr$: C, 33.76; H, 1.89; N, 4.37. Found: C, 33.86; H, 1.96; N, 4.14. High res MS (EI) found (calcd): M^+ 637.9185 (637.9159). The quaternary aryl ^{13}C resonances were not located due to the extremely low solubility of this compound and the presence of solvent aryl resonances.

$Zr[CH_2OCH_2CH_2N(C_6F_5)]_2[N(SiMe_3)_2]Cl$ (4). Method 1: A solution of **1** (0.100 g, 0.208 mmol) and $Zr[N(SiMe_3)_2]_3Cl$ (0.126 g, 0.208 mmol) in toluene (20 mL) was placed in a Schlenk flask sealed with a Kontes valve. The mixture was heated at 110 °C for 3 days with stirring. After cooling, the solvent was removed under vacuum, leaving **4** as a powder. Recrystallization from hot toluene gave white crystals. Yield: 61%. **Method 2:** A toluene solution of $NaN(SiMe_3)_2$ (0.028 g, 0.156 mmol) was added to a suspension of **3** (0.100 g, 0.156 mmol) in toluene with stirring. The cloudy reaction mixture was stirred overnight and filtered through Celite on a sintered glass frit. The filtrate was concentrated and cooled to yield **4** as a white crystalline solid. Yield: 90%. Mp: 230−2 °C. NMR (d_6-benzene): ^1H δ 3.74 (m, 2H, CH_2), 3.57 (m, 2H, CH_2), 3.23 (m, 2H, CH_2), 3.09 (m, 2H, CH_2), 2.72 (m, 4H, CH_2), 0.32 (s, 18H, Si*Me*$_3$); $^{13}C\{^1H\}$ δ 143.8 (d, aryl*C*F, $^1J_{CF} = 237$ Hz), 137.9 (d, aryl*C*F, $^1J_{CF} = 244$ Hz), 134.5 (d, aryl*C*F, $^1J_{CF} = 272$ Hz),

(7) . Zucchini, U.; Albizatti, E.; Giannini, U. *J. Organomet. Chem.* **1971**, *26*, 357.
(8) . Andersen, R. A. *J. Chem. Soc., Dalton Trans.* **1980**, 2010.
(9) Kulstad, S.; Malmsten, L. A. *Acta Chem. Scand. B* **1979**, *33B*, 469.

128.9 (*quat*-aryl*C*), 72.5 (NCH_2CH_2O), 68.1 (OCH_2CH_2O), 54.0 (NCH_2CH_2O)), 4.2 ($SiMe_3$); $^{19}F\{^1H\}$ δ −146.0 (br s, *o*-aryl*F*), −164.4 (t, *p*-aryl*F*, $^3J_{FF}$ = 22.2 Hz), −166.6 (br t, *m*-aryl*F*, $^3J_{FF}$ = 22.2 Hz). $^{29}Si\{^1H\}$ (d_8-toluene): δ −4.21 ppm. Anal. Calcd for the hemi-toluene solvate $C_{27.5}H_{34}N_3O_2F_{10}ClSi_2Zr$: C, 40.71; H, 4.22; N, 5.18. Found: C, 40.59; H, 4.38; N, 5.17.

$Zr[CH_2OCH_2CH_2N(C_6F_5)]_2(CH_2Ph)Cl$ (5). This complex was prepared by the procedure outlined for **3** using equimolar quantities of **1** and $Zr(CH_2Ph)_3Cl$. In this case however, large yellow crystals of **5** were obtained by layering the mother liquor with hexane and cooling at −30 °C. Yield: 63%. Mp: 159−63 °C. NMR (d_5-bromobenzene): ^1H δ 7.1−7.3 (m, 8H, benzyl and toluene H), 6.85 (br m, 2H, benzyl*H*), 4.01 (br m, 2H, CH_2), 3.85 (br s, 2H, CH_2), 3.69 (br m, 2H, CH_2), 3.57 (br s, 2H, CH_2), 3.38 (br s, 2H, CH_2), 3.23 (br s, 2H, CH_2), 2.55 (s, 2H, CH_2Zr); $^{13}C\{^1H\}$ (d_6-benzene) δ 143.4 (*o*- or *m*-aryl*C*F, $^1J_{CF}$ = 254 Hz), 138.5 (*o*- or *m*-aryl*C*F, $^1J_{CF}$ = 254 Hz), 129.3 (*o*- or *m*-benzyl*C*), 128.7 (*o*- or *m*-benzyl*C*), 125.6 (*quat*-benzyl*C*), 121.8 (*p*-benzyl*C*), 73.6 (CH_2Ph), 73.1 (NCH_2CH_2O), 69.8 (OCH_2CH_2O), 53.5 (NCH_2CH_2O). Assignments are tentative; the limited solubility of this compound made it difficult to locate the remaining quaternary aryl resonances. $^{19}F\{^1H\}$ NMR: δ −148.8 (br s, *o*-aryl*F*), −164.0 (t, *p*-aryl*F*, $^3J_{FF}$ = 22.6 Hz), −164.5 (t, *m*-aryl*F* $^3J_{FF}$ = 21.9 Hz).

$Zr[CH_2OCH_2CH_2N(C_6F_5)]_2(CH_2Ph)_2$ (6). Complex **6** was prepared from equimolar quantities of **1** and $Zr(CH_2Ph)_4$ by the procedure described for **3**. Yield: 85%. Mp: 167−9 °C. NMR (d_5-bromobenzene): ^1H δ 7.14 (t, 4H, *m*-aryl*H*, $^3J_{HH}$ = 7.7 Hz), 6.92 (d, 4H, *o*-aryl*H*, $^3J_{HH}$ = 8.1 Hz), 6.80 (t, 2H, *p*-aryl*H*, $^3J_{HH}$ = 7.0 Hz), 3.56 (m, 4H, NCH_2CH_2O), 3.53 (m, 4H, NCH_2CH_2O), 2.82 (s, 4H, OCH_2CH_2O), 2.18 (s, 4H, CH_2Ph); $^{13}C\{^1H\}$ δ 147.6 (*quat*-aryl*C*), 142.3 (d, aryl*C*F, $^1J_{CF}$ = 246 Hz), 138.0 (d, aryl*C*F, $^1J_{CF}$ = 251 Hz), 135.5 (d, aryl*C*F, $^1J_{CF}$ = 280 Hz), 128.2 (*quat*-aryl*C*), 127.6 (*o*- or *m*-benzyl*C*), 127.0 (*o*- or *m*-benzyl*C*), 120.6 (*p*-benzyl*C*), 72.7 (CH_2Ph, t (gated ^{13}C), $^1J_{CH}$ = 124 Hz), 72.0 (NCH_2CH_2O), 68.7 (OCH_2CH_2O), 52.0 (NCH_2CH_2O). Assignments are confirmed by $^1H-^{13}C$ COSY. ^{19}F NMR (d_6-benzene): δ −150.8 (d, *o*-aryl*F*, $^3J_{FF}$ = 21.2 Hz), −164.9 (*m*-aryl*F*, $^3J_{FF}$ = 21.0 Hz), −166.6 (br t, *p*-aryl*F*). ^1H (d_6-benzene): δ 7.16 (t, 4H, *m*-aryl*H*, $^3J_{HH}$ = 7.7 Hz), 7.00 (d, 4H, *o*-aryl*H*, $^3J_{HH}$ = 8.1 Hz), 6.83 (t, 2H, *p*-aryl*H*, $^3J_{HH}$ = 7.0 Hz), 3.26 (m, 4H, NCH_2CH_2O), 3.18 (m, 4H, NCH_2CH_2O), 2.28 (s, 4H, OCH_2CH_2O), 2.22 (s, 4H, CH_2Ph). Anal. Calcd for $C_{32}H_{26}N_2O_2F_{10}Zr$: C, 51.13; H, 3.49; N, 3.72. Found: C, 48.83; H, 3.45; N, 3.77.

$Zr[CH_2OCH_2CH_2N(3,5\text{-}C_6H_3(CF_3)_2)]_2Cl_2$ (7). Complex **7** was prepared from equimolar quantities of **2** and either $Zr[N(SiMe_3)_2]_2Cl_2$ or $Zr(CH_2Ph)_2Cl_2$ using the procedure described for **3**. Pale yellow crystals were obtained by slow cooling of a hot toluene solution to room temperature. Yield: 94%. Mp: 173−5 °C. NMR (d_5-bromobenzene): ^1H δ 7.38 (br s, 6H, *o*- and *p*-aryl*H*), 3.90 (br s, 4H, OCH_2CH_2O), 3.73 (br m, 4H, NCH_2CH_2O), 3.15 (br m, 4H, NCH_2CH_2O); $^{13}C\{^1H\}$ δ 153.5 (*quat*-aryl*C*), 131.6 (q, *m*-aryl*C*, $^2J_{CF}$ = 33 Hz), 123.6 (q, CF_3, $^1J_{CF}$ = 273 Hz), 118.2 (*o*-aryl*C*), 113.7 (*p*-aryl*C*), 75.0 (NCH_2CH_2O), 71.4 (OCH_2CH_2O), 51.8 (NCH_2CH_2O); $^{19}F\{^1H\}$ δ −62.55 (CF_3). Anal. Calcd for $C_{22}H_{18}N_2O_2F_{12}Cl_2Zr$: C, 36.07; H, 2.48; N, 3.82. Found: C, 34.99; H, 2.46; N, 3.85.

$Zr[CH_2OCH_2CH_2N(3,5\text{-}C_6H_3(CF_3)_2)]_2(CH_2Ph)_2$ (8). Yellow-orange crystals of complex **8** were isolated from equimolar quantities of **2** and $Zr(CH_2Ph)_4$ by the procedure described for **3**. Yield: 68%. Mp: 171−4 °C. NMR (d_6-benzene): ^1H δ 7.48 (br s, 2H, *p*-$C_6H_3(CF_3)_2$), 7.42 (br s, 4H, *o*-$C_6H_3(CF_3)_2$), 7.00 (t, 4H, *m*-benzyl*H*, J = 7.4 Hz), 6.76 (br t, 4H, *o*- and *p*-benzyl*H*, J = 7.4 Hz), 2.5−3.0 (br m, 12H, CH_2), 1.94 (br s, 4H, CH_2Ph).; $^{13}C\{^1H\}$ δ 146.7 (*quat*-aryl*C*), 132.4 (q, *m*-aryl*C*, $^2J_{CF}$ = 33 Hz), 130.9 (*quat*-benzyl*C*), 129.2 (*o*- or *m*-benzyl*C*), 128.6 (*o*- or *m*-benzyl*C*), 124.6 (q, CF_3, $^1J_{CF}$ = 233 Hz), 121.4 (*p*-benzyl*C*), 117.1 (*o*-aryl*C*), 112.0 (*p*-aryl*C*), 72.6 (CH_2Ph, t (gated ^{13}C), $^1J_{CH}$ = 124 Hz), 70.7 (NCH_2CH_2O), 67.9 (OCH_2CH_2O), 50.5 (NCH_2CH_2O); $^{19}F\{^1H\}$ δ −62.57 (CF_3). Anal. Calcd for $C_{36}H_{32}N_2O_2F_{12}Zr$: C, 51.24; H, 3.82; N, 3.32. Found: C, 49.55; H, 3.85; N, 3.17.

$\{Zr[CH_2OCH_2CH_2N(C_6F_5)]_2(CH_2Ph)\}^+\{(PhCH_2)B(C_6F_5)_3\}^-$ (9). A solution of $B(C_6F_5)_3$ (0.011 g, 0.020 mmol) in 0.1 mL of CD_2Cl_2 was added to a precooled (−30 °C) solution of **6** (0.015 g, 0.021 mmol) in 0.4 mL of CD_2Cl_2 in the glovebox. The deep orange solution was thoroughly mixed and allowed to stand at room temperature for 10 min. The product was characterized in situ by NMR spectroscopy; degradation of the sample was observed over 4 h. ^1H NMR: δ 7.52 (t, 2H, *m*-aryl*H*), 7.32 (t, 1H, *p*-arylH), 6.98 (d, 2H, *o*-aryl*H*), 6.87 (t, 2H, *m*-aryl*H*), 6.79 (t, 1H, *p*-aryl*H*), 6.73 (d, 2H, *o*-aryl*H*), 4.54 (dt, 2H, CH_2, J = 9.5, 4.8 Hz), 4.27 (dt, 2H, CH_2, J = 9.5, 5.0 Hz), 4.17 (m, 2H, CH_2), 4.04 (br t, 4H, CH_2, J = 5.0 Hz), 3.90 (m, 2H, CH_2), 2.81 (s, 2H, $ZrCH_2$), 2.77 (br s, 2H, BCH_2). $^{13}C\{^1H\}$ NMR: δ 132.7, 130.0, 129.0, 128.7, 127.3, 122.9 (aryl*C*H), 79.3 (NCH_2CH_2O), 75.2 ($ZrCH_2Ph$, t (gated ^{13}C), $^1J_{CH}$ = 138 Hz), 73.2 (OCH_2CH_2O), 60.8 (BCH_2Ph), 52.9 (NCH_2CH_2O). The quaternary aryl carbon resonances were not observable. $^{19}F\{^1H\}$ NMR: δ −132.0 (d, 6F, borate *o*-aryl*F*, $^3J_{FF}$ = 23.4 Hz), −150.4 (d, 4F, ligand *o*-aryl*F*, $^3J_{FF}$ = 23.2 Hz), −162.4 (dt, 4F, ligand *m*-aryl*F*, J_{FF} = 22.5, 3.5 Hz), −165.0 (t, 3F, borate *p*-aryl*F*, $^3J_{FF}$ = 20.4 Hz), −165.4 (t, 2F, ligand *p*-aryl*F*, $^3J_{FF}$ = 21.6 Hz), −168.1 (t, 6F, borate *m*-aryl*F*, $^3J_{FF}$ = 19.6 Hz). $^{11}B\{^1H\}$ NMR: δ −10.9 (s).

In a second experiment, a sample of **9** was prepared exactly as above except that 0.1 mL of d_8-THF was added to the sample prior to recording the NMR spectra. ^1H NMR: δ 7.00 (t, 2H, *m*-aryl*H*), 6.90 (t, 2H, *m*-aryl*H*), 6.81 (m, 3H, overlapping *o,p*-aryl*H*), 6.75 (m, 3H, *o,p*-aryl*H*), 4.54 (br m, 2H, CH_2), 4.49 (br m, 2H, CH_2), 4.40 (br m, 2H, CH_2), 4.25 (s, 2H, CH_2), 4.15 (br m, 2H, CH_2), 4.06 (br m, 2H, CH_2), 2.80 (br s, 2H, BCH_2), 2.49 (s, 2H, $ZrCH_2$). $^{13}C\{^1H\}$ NMR: δ 79.6 (NCH_2CH_2O), 75.1 (OCH_2CH_2O), 73.7 ($ZrCH_2Ph$, t (gated ^{13}C), $^1J_{CH}$ = 126 Hz), 53.0 (NCH_2CH_2O). The aryl carbon resonances occur between 122 and 152 ppm. $^{19}F\{^1H\}$ NMR: δ −129.8 (d, 6F, borate *o*-aryl*F*), −148.5 (d, 4F, ligand *o*-aryl*F*), −161.5 (t, 4F, ligand *m*-aryl*F*), −162.9 (t, 3F, borate *p*-aryl*F*), −165.6 (br m, 2F, ligand *p*-aryl*F*), −165.9 (br s, 6F, borate *m*-aryl*F*).

Olefin Polymerization Tests. A solution of **3** (0.040 g, 0.062 mmol) in toluene (30 mL) was placed in a Schlenk flask equipped with a Kontes valve and degassed by three freeze−pump−thaw cycles. The solution was placed under 1 atm of ethylene, MAO (20 mL of a 10% by wt solution in toluene, ca. 500 equiv) was added, and the sealed flask was immersed in a 50 °C oil bath for 1 h with rapid stirring. At the end of this period, methanol (12 mL) was added to the flask and the precipitated solids were dried on the vacuum line. The solids were stirred in aqueous HCl (20%) overnight, collected by filtration, and washed with water and then hexanes. The remaining solid was dried under vacuum to yield polyethylene (0.199 g; rate = 3.2 kg mol^{-1} Zr h^{-1}). A blank experiment run with only MAO produced no polyethylene under these conditions.

X-ray Crystallographic Studies. Crystallographic data for **1**, **4**, **5**, and **7** are given in Table 1. A crystal of **1** was grown from a saturated hexane solution at −30 °C; crystals of **4**, **5**, and **7** were obtained by cooling a warm (60 °C) toluene solution to room temperature. Crystals of **4**, **5**, and **7** were loaded into glass capillaries in the glovebox while crystals of **1** were mounted on a glass fiber in air. The crystals were transferred to a Nonius CAD4F diffractometer equipped with Cu Kα or Mo Kα radiation. The unit cells were refined using 25 reflections in the 2θ range 59−64° (**4**), 70−80° (**5**), 36−40° (**1**), and 32−44° (**7**). Experimental densities were not determined. From three to six standard reflections, measured at 1 h intervals during data collection, showed less than a 2% decline in combined intensity for **1**, **5**, and **7**; however, the standards for **4** decayed to 59.9% of their original intensity so a decay correction was applied. Intensity measurements were collected for one-half of the sphere for **1** and **5** and one-fourth of the

Table 1. Summary of Crystallographic Data

	1	4	5	7
formula	$C_{18}H_{14}N_2O_2F_{10}$	$C_{24}H_{30}N_3O_2F_{10}ClSi_2Zr\cdot 1/2C_7H_8$	$C_{25}H_{19}N_2O_2F_{10}ClZr\cdot 1/2C_7H_8$	$C_{22}H_{18}N_2O_2F_{12}Cl_2Zr$
fw	480.29	811.40	742.15	732.49
cryst syst	triclinic	monoclinic	triclinic	monoclinic
space group	$P\bar{1}$ (No. 2)	$P2_1/n$ (No. 14)	$P\bar{1}$ (No. 2)	$P2_1/c$ (No. 14)
a (Å)	7.022(3)	12.815(1)	7.4451(6)	8.560(1)
b (Å)	9.601(2)	18.883(2)	11.558(2)	18.381(3)
c (Å)	15.121(4)	14.915(2)	17.514(2)	17.260(2)
α (deg)	87.48(2)	90	94.850(12)	90
β (deg)	77.73(2)	103.226(9)	94.790(9)	94.166(11)
γ (deg)	73.54(2)	90	93.639(10)	90
V (Å^3)	955.1(5)	3513.3(6)	1492.7(3)	2708.5(6)
Z	1	4	2	4
ρ(calcd) (g cm^{-3})	1.67	1.54	1.55	1.80
μ (cm^{-1})	1.75	47.69	47.56	7.10
λ (Å)	Mo Kα, 0.7107	Cu Kα, 1.542	Cu Kα, 1.542	Mo Kα, 0.7107
T	ambient	ambient	ambient	ambient
$2\theta_{max}$ (deg)	45	120	120	45
no. of obsd reflns	2740	5574	4433	3807
no. of unique reflns	2497	5351	4372	3671
F_{000}	484	1648	692	1448
R^a	0.064	0.048	0.069	0.058
$R_w{}^b$	0.047	0.039	0.057	0.044

[a] $R = \sum(|F_o| - |F_c|)/\sum|F_o|$. [b] $R_w = [\sum w(|F_o| - |F_c|^2)/\sum w(|F_o|)^2]^{1/2}$.

sphere for **4** and **7**. After the usual data reduction procedures (NRCVAX),[10] the structures were solved using the Patterson[11] or direct methods (SIR97)[12] options in teXsan98.[13] Structure expansion was carried out using Fourier synthesis, and the least-squares refinements minimized $\sum w((|F_o| - |F_c|)^2)$.[14] The criterion for inclusion of reflections was $I > 2.5\sigma(I)$ for **1**, $I > 3.0\sigma(I)$ for **4** and **7**, and $I > 4.0\sigma(I)$ for **5**. The weighting scheme was determined by counting statistics using $w = 1/\sigma^2(F) + 0.001(F^2)$. The data were corrected for absorption and Lorentz−polarization, and the secondary extinction coefficient was refined in all cases. The toluene of solvation in **4** lies on a special position so that the methyl group is disordered about the 2_1 screw axis. The methyl group was modeled successfully as half-occupancy over both sites. Similarly, **5** contains a half molecule of toluene per formula unit. In this case, the toluene was modeled as a rigid C_7H_5 group and refined isotropically with a single group thermal parameter and occupancy factor. The occupancy factor refined to 0.531, consistent with our observation of half-equivalent of toluene by NMR spectroscopy. For **7**, two of the four CF_3 groups were disordered. Ultimately the best refinement was achieved by refining all atoms anisotropically while restraining the C−F bond distances to 1.30 Å for the two disordered CF_3 groups (C14/F4,F5,F6 and C22/F10,F11,F12). The largest positive and negative peaks in the final Fourier difference map were rather large for this structure (1.28 and −1.09 e/Å^3) and were associated with the disordered CF_3 groups. Structural plots were drawn with ORTEP3.[15]

(10) Larson, A.; Lee, F.; Page, Y.; Webster, M.; Charland, J.; Gabe, E. J. *NRC Solver*: A Program for Crystal Structure Determination; National Research Council of Canada, Chemistry Division: Ottawa, 1985.

(11) Beurskens, P. T.; Admiraal, G.; Beurskens, G.; Bosman, W. P.; Garcia-Granda, S.; Gould, R. O.; Smits, J. M. M.; Smykalla, C. *ORIENT*: Technical Report of the Crystallography Laboratory; University of Nijmegen: The Netherlands, 1992.

(12) Altomare, A.; Cascarano, M.; Giacovazzo, C.; Guagliardi, A. SIR97. *J. Appl. Crystallogr.* **1993**, *26*, 343.

(13) *teXsan for Windows*: *Crystal Structure Analysis Package*; Molecular Structure Corporation, 1997.

(14) Beurskens, P. T.; Admiraal, G.; Beurskens, G.; Bosman, W. P.; de Gelder, R.; Israel, R.; Smits, J. M. M. *DIRDIF94*; Technical Report of the Crystallography Laboratory; University of Nijmegen: The Netherlands, 1994.

(15) Farrugia, L. J. ORTEP3 for Windows. *J. Appl. Crystallogr.* **1997**, *30*, 565.

Results

The fluorinated diamines **1** and **2** were prepared in moderate yield by reaction of 1,2-bis(2-iodoethoxy)-ethane with an excess of the aniline anion, formed by in situ deprotonation of the commercially available fluorinated aniline with *n*-BuLi (eq 1). An excess of

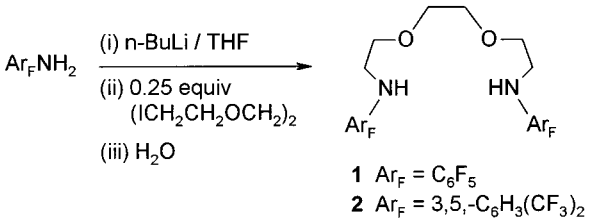

(1)

1 $Ar_F = C_6F_5$

2 $Ar_F = 3,5\text{-}C_6H_3(CF_3)_2$

fluorinated aniline anion was necessary in order to obtain acceptable yields, but it is possible to recover the volatile anilines by short-path vacuum distillation after quenching the reaction mixture with water. The amines were isolated as nearly white crystals by extraction of the tarry residue with ether and repeated recrystallization from hexanes. Crystals of **1** obtained in this manner were suitable for X-ray diffraction (Table 1). The solid state structure of this diamine shows a fully extended, ladder-like backbone chain with π-stacking between the fluorinated aryl groups of adjacent molecules (Figure 1).

Zirconium complexes containing fluorinated amide ligands were synthesized by direct protonolysis of a suitable zirconium precursor with amines **1** and **2** (eqs 2−4). The benzyl and silylamido zirconium derivatives, $Zr(CH_2Ph)_nCl_{4-n}$ ($n = 2-4$) and $Zr[N(SiMe_3)_2]_nCl_{4-n}$ ($n = 2-3$), are ideally suited to this purpose. In general, we have found that metathesis of zirconium chlorides with the dilithium salts of the amides produces poorer yields and less pure materials than the protonolysis route.[5,6] However, the mixed silylamide chloride complex **4** can be conveniently prepared from **3** and 1 equiv

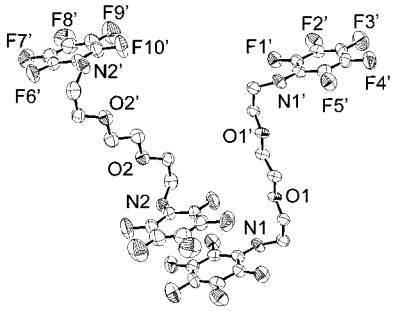

Figure 1. ORTEP3 drawing[15] (thermal ellipsoid 30% probability) of diamine **1**.

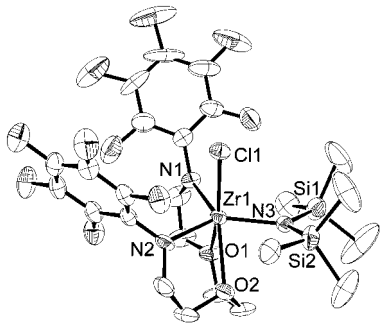

Figure 2. ORTEP3 drawing[15] (thermal ellipsoid 30% probability) of complex **4**. The toluene of solvation (1/2 molecule) is omitted for clarity.

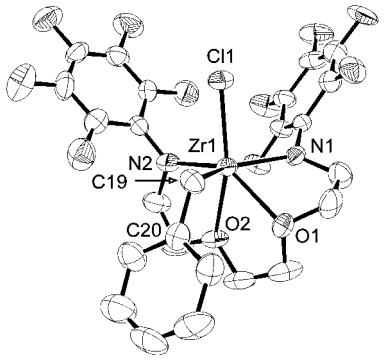

Figure 3. ORTEP3 drawing[15] (thermal ellipsoid 30% probability) of complex **5**. The toluene of solvation (1/2 molecule) is omitted for clarity.

of $NaN(SiMe_3)_2$ (eq 5), presumably because the large silylamido group prevents unwanted side reactions (for

1 or **2** + ZrL_2Cl_2 $\xrightarrow{-2\ HL}$ $Zr\{Ar_FNCH_2CH_2OCH_2\}_2Cl_2$ (2)

3 $Ar_F = C_6F_5$
7 $Ar_F = 3,5\text{-}C_6H_3(CF_3)_2$

1 or **2** + $Zr(CH_2Ph)_4$ $\xrightarrow{-2\ C_7H_8}$ $Zr\{Ar_FNCH_2CH_2OCH_2\}_2(CH_2Ph)_2$ (3)

6 $Ar_F = C_6F_5$
8 $Ar_F = 3,5\text{-}C_6H_3(CF_3)_2$

1 + ZrL_3Cl $\xrightarrow{-2\ HL}$ $Zr\{(C_6F_5)NCH_2CH_2OCH_2\}_2(L)(Cl)$ (4)

4 $L = N(SiMe_3)_2$
5 $L = CH_2Ph$

$Zr\{(C_6F_5)NCH_2CH_2OCH_2\}_2Cl_2$ + $NaN(SiMe_3)_2$ $\xrightarrow{-NaCl}$ (5)

$Zr\{(C_6F_5)NCH_2CH_2OCH_2\}_2\{N(SiMe_3)_2\}Cl$

4

example, formation of the complex with two silylamido ligands). All of the complexes were isolated as white or very pale yellow crystals except those containing benzyl groups, which were yellow-orange in color. With the exception of **4**, complexes containing chloride ligands (**3**, **5**, and **7**) displayed much lower solubility than the dibenzyl derivatives (**6** and **8**). While this might be taken as evidence of bridging halide interactions between monomeric units, we do not believe this to be the case. The solid state structures of **5** and **7** have both been determined (vide infra), and there is no evidence for significant intermolecular interactions; complex **5** is in fact distorted toward a five-coordinate structure, so it is highly unlikely that any bridging halide interactions persist in solution. Of further note, **3** readily gives a monomeric molecular ion in the mass spectrum, and while this is not definitive proof that the solution or solid state species are monomeric in nature, it has been our experience that this is usually the case.

The solid state structures of the mixed ligand chloro complexes **4** and **5** were determined by X-ray crystallography (Table 1). The structures are depicted in Figures 2 and 3, while important bond distances and angles are summarized in Table 2. Both complexes contain a six-coordinate zirconium center in what is best described as a capped trigonal bipyramidal geometry. In each structure, the amido nitrogens of the chelating ligand and the silylamido (**4**) or benzyl (**5**) groups are located in equatorial positions, while the axial sites are occupied by the chloro group and one ether oxygen. This arrangement, where the bulkier ligand occupies the equatorial site, is typical of trigonal bipyramidal mixed-ligand complexes.[4c,d] The other ether oxygen caps one face of the trigonal bipyramid. The bond angles around zirconium in the equatorial plane sum to 360.0° in both structures, indicating that the zirconium lies in the trigonal plane. As might be expected, the angle between the chelating amido nitrogens is significantly compressed when the other equatorial group is a bulky silylamide (**4**, 104.9(3)°) versus a benzyl group (**5**, 121.1(2)°). In both structures, the two angles between the chelating amido nitrogens and the other equatorial substituent are highly asymmetric (**4**, 120.6(3)° and 134.5(3)°; **5**, 103.4(2)° and 135.5(2)°), the wider angle being on the side with the capping oxygen. Thus these structures can be viewed as distortions from an octahedral geometry where one oxygen is forced out of the equatorial plane and away from the metal due to steric crowding.

The Zr−Cl and Zr−N bond distances in **4** and **5** are very similar to one another, while the Zr−O distances are greater in the more crowded silylamide complex **4**. The axial Zr−O bond is nearly 0.1 Å shorter than the Zr−O capping oxygen distance in both compounds. The most closely related structures reported in the literature are the *fac*-trigonal bipyramidal Zr complexes bearing *NON*-,[4f] *NSN*-,[4a,d] *NNN*-,[16] and *NPN*-type[4c] chelate ligands and the six-coordinate complexes $ZrCl_2(NR_2)_2(THF)_2$ (R = Me, Et)[17] which contain *trans*-

Table 2. Selected Bond Distances (Å) and Angles (deg) for Zirconium Complexes 4, 5, and 7[a]

4		5		7	
		Distances			
Zr(1)−Cl(1)	2.461(2)	Zr(1)−Cl(1)	2.431(3)	Zr(1)−Cl(1)	2.427(2)
Zr(1)−O(1)	2.296(4)	Zr(1)−O(1)	2.347(8)	Zr(1)−Cl(2)	2.417(2)
Zr(1)−O(2)	2.372(5)	Zr(1)−O(2)	2.276(7)	Zr(1)−O(1)	2.263(4)
Zr(1)−N(1)	2.102(5)	Zr(1)−N(1)	2.076(9)	Zr(1)−O(2)	2.294(4)
Zr(1)−N(2)	2.131(5)	Zr(1)−N(2)	2.076(10)	Zr(1)−N(1)	2.101(5)
Zr(1)−N(3)	2.100(5)	Zr(1)−C(19)	2.292(11)	Zr(1)−N(2)	2.120(5)
		Angles			
Cl(1)−Zr(1) −O(1)	155.3(1)	Cl(1)−Zr(1)−O(1)	129.1(2)	Cl(1)−Zr(1)−Cl(2)	92.42(7)
Cl(1)−Zr(1)−O(2)	138.7(1)	Cl(1)−Zr(1)−O(2)	162.3(2)	Cl(1)−Zr(1)−O(1)	91.93(13)
Cl(1)−Zr(1)−N(1)	85.5(2)	Cl(1)−Zr(1)−N(1)	89.4(3)	Cl(1)−Zr(1)−O(2)	81.90(12)
Cl(1)−Zr(1)−N(2)	90.7(2)	Cl(1)−Zr(1)−N(2)	90.5(3)	Cl(1)−Zr(1)−N(1)	102.5(2)
Cl(1)−Zr(1)−N(3)	92.7(1)	Cl(1)−Zr(1)−C(19)	87.0(3)	Cl(1)−Zr(1)−N(2)	147.2(2)
O(1)−Zr(1)−O(2)	65.9(2)	O(1)−Zr(1)−O(2)	68.6(3)	Cl(2)−Zr(1)−O(1)	166.17(12)
O(1)−Zr(1)−N(1)	70.4(2)	O(1)−Zr(1)−N(1)	68.9(3)	Cl(2)−Zr(1)−O(2)	126.63(12)
O(1)−Zr(1)−N(2)	99.8(2)	O(1)−Zr(1)−N(2)	140.3(3)	Cl(2)−Zr(1)−N(1)	94.4(1)
O(1)−Zr(1)−N(3)	95.5(2)	O(1)−Zr(1)−C(19)	79.0(4)	Cl(2)−Zr(1)−N(2)	87.1(2)
O(2)−Zr(1)−N(1)	133.6(2)	O(2)−Zr(1)−N(1)	97.5(3)	O(1)−Zr(1)−O(2)	67.0(2)
O(2)−Zr(1)−N(2)	69.1(2)	O(2)−Zr(1)−N(2)	71.9(3)	O(1)−Zr(1)−N(1)	71.8(2)
O(2)−Zr(1)−N(3)	78.9(2)	O(2)−Zr(1)−C(19)	99.3(4)	O(1)−Zr(1)−N(2)	96.3(2)
N(1)−Zr(1)−N(2)	104.8(2)	N(1)−Zr(1)−N(2)	121.7(4)	O(2)−Zr(1)−N(1)	138.8(2)
N(1)−Zr(1)−N(3)	120.8(2)	N(1)−Zr(1)−C(19)	134.9(4)	O(2)−Zr(1)−N(2)	72.4(2)
N(2)−Zr(1)−N(3)	134.4(2)	N(2)−Zr(1)−C(19)	103.3(4)	N(1)−Zr(1)−N(2)	110.2(2)
Zr(1)−N(1)−C(1)	122.9(5)	Zr(1)−N(1)−C(1)	126.2(8)	Zr(1)−N(1)−C(1)	117.9(4)
Zr(1)−N(1)−C(7)	128.0(4)	Zr(1)−N(1)−C(7)	120.8(7)	Zr(1)−N(1)−C(7)	128.6(4)
Zr(1)−N(2)−C(6)	122.6(5)	Zr(1)−N(2)−C(6)	119.9(8)	Zr(1)−N(2)−C(6)	115.4(4)
Zr(1)−N(2)−C(13)	123.1(4)	Zr(1)−N(2)−C(13)	127.6(8)	Zr(1)−N(2)−C(15)	125.6(4)
Zr(1)−N(3)−Si(1)	123.7(3)	Zr(1)−C(19)−C(20)	117.9(8)	C(1)−N(1)−C(7)	113.3(5)
Zr(1)−N(3)−Si(2)	117.9(3)			C(6)−N(2)−C(15)	114.1(6)

[a] Estimated standard deviations in parentheses.

chloro, *cis*-amido, and *cis*-tetrahydrofuran groups. In these structures the Zr−N and Zr−C bond lengths span the ranges 2.054(3)−2.116(2) and 2.278(2)−2.343(8) Å, respectively.[4a,c,d,f] The Zr−N bond lengths in **4** and **5** (2.100(6)−2.124(7) Å) and the Zr−C bond in **5** (2.363(7) Å) are at the long end of this range, consistent with a more crowded six-coordinate geometry. The Zr−Cl distances in **4** and **5** (2.462(2) and 2.431(3) Å, respectively) are similar to those observed for the six-coordinate complexes $ZrCl_2(NR_2)_2(THF)_2$ (2.486−2.487 Å)[17] and for the axial Zr−Cl distances in the *fac-tbp* structures {(*t*-BuN-*o*-$C_6H_4)_2S$}ZrCl(NMe_2) (2.4555(11) Å),[4d] {(*t*-$BuNCH_2CH_2)_2PPh$}ZrCl(Me) (2.5067(6) Å),[4c] and the six-coordinate dimer [{(*t*-BuN-*o*-$C_6H_4)_2O$}ZrCl-(μ-Cl)]$_2$ (2.40125(13) Å).[4f]

The structure of **7** was also determined by X-ray crystallography. The structure is shown in Figure 4, and significant bond lengths and angles are collected in Table 2. This complex also adopts a structure that can be viewed as a capped trigonal biypramid, although the distortions from an octahedral geometry are noticeably less pronounced in **7** than for **4** or **5**. This is most evident in the less asymmetric Zr−O bond lengths (Δ = (Zr−O_{cap})−(Zr−O_{axial}) = 0.031 Å). The Zr−Cl distances are slightly shorter in **7** than in **4** or **5**, while the Zr−N distances are essentially the same in all three compounds. Not surprisingly, these observations are consistent with less steric crowding in **7** than in **4** or **5**. Interestingly, **7** adopts an extended lattice structure with π-stacking between the $C_6H_3(CF_3)_2$ rings of adjacent molecules (Figure 5). The limited solubility of **7** may stem from the strength of these interactions since no intermolecular interactions involving the chloro ligands are observed.

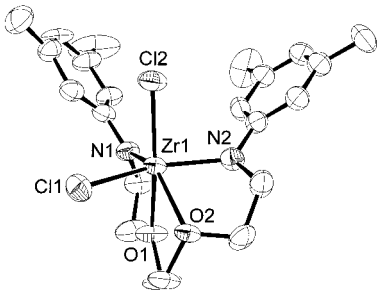

Figure 4. ORTEP3 drawing[15] (thermal ellipsoid 30% probability) of complex **7**. The fluorines of the CF_3 groups have been omitted for clarity.

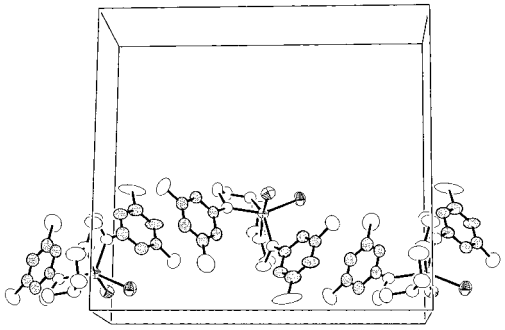

Figure 5. ORTEP3 packing diagram[15] showing π-stacking interactions between the $C_6H_3(CF_3)_2$ rings (shaded) in adjacent molecules. Only one of the two chains passing through the unit cell is shown. Fluorines of the CF_3 groups have been omitted for clarity.

The ^{1}H NMR spectra of the mixed-ligand complexes **4** and **5** show higher symmetry in solution than is

(16) (a) Cloke, F. G. N.; Hitchcock, P. B.; Love, J. B. *J. Chem. Soc., Dalton Trans.* **1995**, 25. (b) Horton, A. D.; de With, J.; van der Linden, A. J.; van de Weg, H. *Organometallics* **1996**, *15*, 2672.

(17) Brenner, S.; Kempe, R.; Arndt, P. *Z. Anorg. Allg. Chem.* **1995**, *621*, 2021.

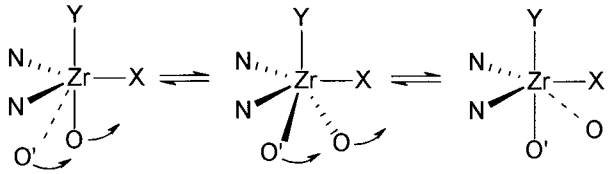

Figure 6. Axial-capping oxygen exchange for a six-coordinate, capped-*tbp* structure.

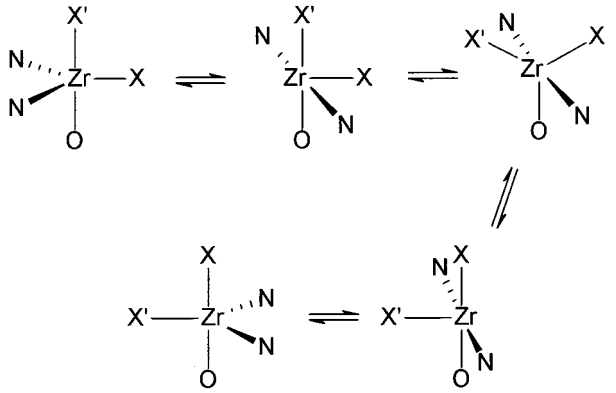

Figure 7. Backbone inversion of a five-coordinate intermediate derived from **3** and **6**−**8**.

observed in the crystal structure. The observation of only six backbone CH_2 resonances, rather than 12, indicates average C_s symmetry in solution. This fact can be accommodated by a simple shift of the ether oxygens between the capping and axial positions such that an average mirror plane passes through the midpoint of the OCH_2CH_2O carbon−carbon bond and between the two aryl amido groups (Figure 6). Similarly, the ^1H NMR spectra of **3**, **6**, **7**, and **8** all show three backbone CH_2 resonances at room temperature, indicating that a fluxional process (or processes) is also operative for these complexes. While the solid state structures of **3**, **6**, and **8** are not known, its seems reasonable to postulate that they adopt a capped trigonal bipyramidal geometry similar to **4**, **5**, and **7**. If this is correct, then the structures would have no symmetry and 12 resonances would be expected. Given the weak binding of one oxygen donor evident in the solid state, it is reasonable to assume that ether oxygen dissociation occurs to give a five-coordinate species that undergoes backbone inversion (Figure 7). If this process and the axial-capping oxygen interchange depicted in Figure 6 are both fast on the NMR time scale, then average C_{2v} symmetry is obtained and only three backbone resonances should be observed. The trigonal biyramidal complex $[\{(2,6\text{-}Me_2C_6H_3)NCH_2CH_2\}_2O]Ti(CH_2Ph)_2$ has a structure analogous to **4** and **5** (without the capping oxygen), and it too undergoes a similar fluxional process, albeit at a slower rate.[4j] The larger size of zirconium compared to titanium may be responsible for the faster rate observed here. Similarly, the complexes $[\{(2,6\text{-}Me_2C_6H_3)NCH_2CH_2\}_2O]ZrX_2$ (X = NMe_2 or Me) adopt a *fac*-trigonal bipyramidal geometry, and they too display an average C_{2v} structure in solution on heating (100 °C, X = NMe_2; 60 °C, X = Me).[4a,d] While it is quite reasonable to assume that **4** and **5** also undergo backbone inversion (Figure 7), it is not possible to distinguish this possibility by NMR.

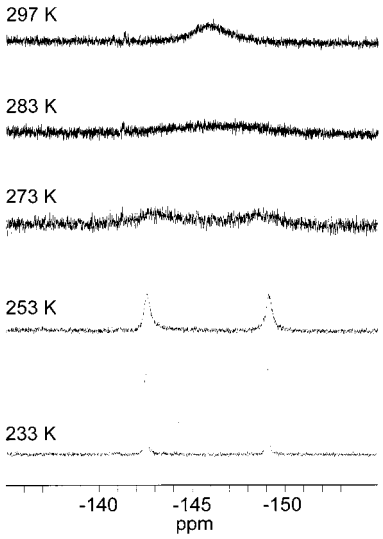

Figure 8. Variable-temperature $^{19}F\{^1H\}$ NMR spectra (d_5-bromobenzene) for the *ortho*-F resonances of **4**.

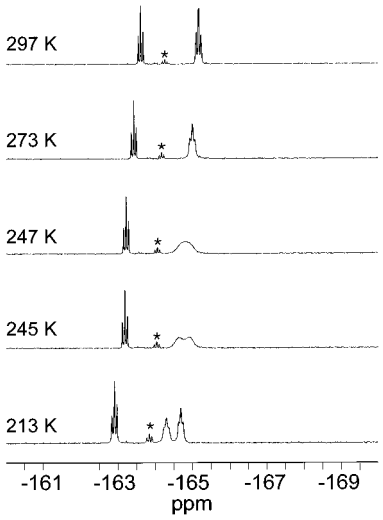

Figure 9. Variable-temperature $^{19}F\{^1H\}$ NMR spectra (d_5-bromobenzene) for the *meta*- and *para*-F resonances of **4** (∗ marks an impurity).

The ^{19}F NMR spectrum of **4** shows evidence for restricted rotation of the C_6F_5 rings. At room temperature the *ortho*-F resonance at δ −146.0 ppm is severely broadened, but on cooling it decoalesces into two signals separated by nearly 7 ppm (Figure 8). The *meta*-F shows similar behavior, while the *para*-F remains a simple triplet over the entire temperature range (Figure 9). From the coalescence temperatures in Figures 8 and 9, the activation energy for this process is calculated to be 49 ± 3 kJ/mol.[18] None of the other complexes show any evidence for restricted rotation of the amido aryl rings, suggesting that steric interference between the bulky silylamido group and the aryl rings is responsible for this effect. Restricted rotation about the $N-C_{ipso}$ aryl bond has been observed for several zirconium complexes

(18) (a) The free energy of activation was calculated from the coalescence temperature (T_c) using the equal population, two-site exchange equation: $\Delta G^{\ddagger} = (1.912 \times 10^{-2})(T_c)[9.972 + \log(T_c/\delta\nu)]$ in kJ mol^{-1} where $\delta\nu$ is the separation of the resonances in Hz at coalescence and T_c is in K.[19b] The error in $\Delta G^{\ddagger}$ was estimated to be ±3 kJ mol^{-1} assuming a liberal error of ±3 °C in estimation of T_c. (b) Sandstrom, J. *Dynamic NMR Spectroscopy*; Pergamon: London, 1982.

bearing diamido ligands that contain bulky 2,6-diisopropylphenyl groups on nitrogen.[3a,e,4e,j]

The benzyl complexes **5**, **6**, and **8** do not show any of the NMR features normally associated with η^2-benzyl bonding.[19] For example, the *ortho*-benzyl protons do not appear upfield of 6.7 ppm (**5**, 6.85; **6**, 6.92; **8**, 6.76 ppm), and the $^1J_{CH}$ coupling constants for the benzyl CH_2 groups are less than 130 Hz (**6**, 124 Hz). In addition, the crystal structure of **5** shows unequivocally that this complex possesses a η^1-benzyl group ($Zr-CH_2-C_{ipso}$ angle = 120.6(4)°).

Complexes **3** and **6** were examined as precatalysts for olefin polymerization. A mixture of **3** and 500 equiv of MAO showed modest activity for the polymerization of ethylene (1 atm, 3.2 kg mol^{-1} Zr h^{-1}) at 50 °C. Treatment of dibenzyl complex **6** with 1 equiv of $B(C_6F_5)_3$ in d_2-dichloromethane resulted in an orange solution, which was inactive as a polymerization catalyst for 1-hexene or ethylene. The NMR data strongly support benzyl abstraction[20] to produce $\{Zr[CH_2OCH_2CH_2N(C_6F_5)]_2(CH_2Ph)\}^+\{(PhCH_2)B(C_6F_5)_3\}^-$ (**9**); however, it is less clear from this evidence alone whether strong anion coordination occurs in d_2-dicloromethane solution.[21] There is evidence for η^2-benzyl coordination to zirconium ($^1J_{CH}$ = 138 Hz for the benzyl CH_2 group) in **9**, although the *o*-benzyl protons do not appear as far upfield as might be expected.[19] Addition of d_8-THF to a d_2-dichloromethane solution of **9** has little effect on the borate anion ^{19}F resonances, but it does result in a significant change in the ^1H chemical shift (2.41 ppm) and $^1J_{CH}$ coupling constant ($^1J_{CH}$ = 126 Hz) associated with the Zr-CH_2Ph group. From these observations we conclude that in noncoordinating solvents **9** most likely exists as a weakly associated anion−cation pair with the cation containing an η^2-benzyl group (eq 6).

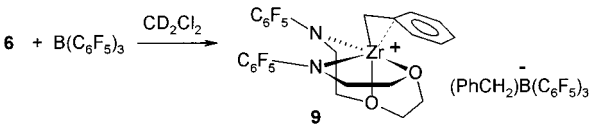

(6)

Discussion

The solid state structures of **7**, **5**, and **4**, taken in that order, show increasing distortion away from an octahedron and toward a highly asymmetric capped trigonal bipyramidal geometry. This is evident from the increasing dihedral angle between the capping oxygen and the plane containing the three equatorial ligands (**7**, 52.9°; **5**, 59.4°; **4**, 62.6°) and from the displacement of the capping oxygen from the same plane (**7**, 1.46 Å; **5**, 1.58 Å; **4**, 1.66 Å). This is accompanied by increasing asymmetry in the Zr−O bond lengths ($\Delta = (Zr-O_{cap})-(Zr-O_{axial})$: **7**, 0.031 Å; **5**, 0.071 Å; **4**, 0.076 Å). This effect would appear to be primarily steric in origin, as the size of the other equatorial ligand increases in the order Cl (**7**) < CH_2Ph (**5**) < $N(SiMe_3)_2$ (**4**). The observation of hindered $N-C_{aryl}$ ring rotation in **4** also supports a high degree of crowding in this complex. There does not appear to be a large difference in steric profile between the C_6F_5 and 3,5-$C_6H_3(CF_3)_2$ aryl groups given the small size of fluorine and the *meta*-CF_3 disposition. However, since we were unable to obtain structural information for **3** (the structural pair of **7**), we cannot establish the extent to which electronic differences between the C_6F_5 and 3,5-$C_6H_3(CF_3)_2$ ligands play a role.

Not surprisingly, given the evidence for η^2-benzyl coordination, treatment of **6** with 1 equiv of $B(C_6F_5)_3$ does not produce an active catalyst for ethylene or 1-hexene polymerization. Even using 500 equiv of MAO as initiator, **3** displays modest activity for ethylene polymerization at 50 °C. In hindsight, this result is consistent with Schrock's postulate that the 12e five-coordinate $M(NON)R_2$ species must generate a 10e four-coordinate, cationic metal center $M(NON)R^+$ in order to bind and insert hexene or ethylene.[4a] No olefin polymerization activity was observed when 1 equiv of Et_2O was coordinated to the cationic metal center, presumably because the ether base was not labile. The ligand systems described in this work possess a second *built-in* ether donor, so formation of a complex with less than a 12e cationic metal center is unlikely. Thus, the systems described here do not appear to be well-suited to olefin polymerization chemistry.

The fluorinated amido ligands do impart high Lewis acidity to the metal center in these complexes. This is demonstrated by the rapid polymerization of ethyl vinyl ether by **3**[22] and by η^2-coordination of the benzyl group in the cation of **9**. Work is continuing to investigate the use of these complexes as Lewis acid catalysts.

Acknowledgment. The support of the Natural Sciences and Engineering Research Council of Canada is gratefully acknowledged. The authors would like to thank one referee for valuable comments.

Supporting Information Available: Tables of atomic coordinates, bond distances and angles, and anisotropic thermal parameters for **1**, **4**, **5** and **7**. This material is available free of charge via the Internet at http://pubs.acs.org.

OM0006559

(19) (a) Latesky, S. L.; McMullen, A. K.; Niccolai, G. P.; Rothwell, I. P.; Huffman, J. C. *Organometallics* **1985**, *4*, 902. (b) Bochmann, M.; Lancaster, S. J. *Organometallics* **1993**, *12*, 633. (c) Bochmann, M.; Lancaster, S. J.; Hursthouse, M. B.; Malik, K. M. A. *Organometallics* **1994**, *13*, 2235. (d) Jordan, R. F.; LaPointe, R. E.; Bajgur, C. S.; Echolls, S. F.; Willet, R. *J. Am. Chem. Soc.* **1987**, *109*, 4111.

(20) Conversion of neutral $B(C_6F_5)_3$ to a borate $B(CH_2Ph)(C_6F_5)_3^-$ is clear from the upfield shift of the ^{11}B resonance from +60.1 to −10.9 ppm (d_2-dichloromethane).

(21) It has been suggested that a $\Delta\delta_{m,p}$ value of greater than 3.0 ppm is indicative for strong anion binding.[16b] The value observed for **9** is 3.0 ppm versus a typical free anion value of 2.6 ppm.

(22) Steeves, S.; Berg, D. J. Unpublished results.